

On the computation of long-range interactions in fluids under confinement: Application to pore systems with various types of spatial periodicity

Evangelia Pantatosaki and George K. Papadopoulos

Citation: *J. Chem. Phys.* **127**, 164723 (2007); doi: 10.1063/1.2799986

View online: <http://dx.doi.org/10.1063/1.2799986>

View Table of Contents: <http://jcp.aip.org/resource/1/JCPSA6/v127/i16>

Published by the [American Institute of Physics](#).

Additional information on *J. Chem. Phys.*

Journal Homepage: <http://jcp.aip.org/>

Journal Information: http://jcp.aip.org/about/about_the_journal

Top downloads: http://jcp.aip.org/features/most_downloaded

Information for Authors: <http://jcp.aip.org/authors>

ADVERTISEMENT



HAVE YOU HEARD?

Employers hiring scientists
and engineers trust
physicstoday JOBS



<http://careers.physicstoday.org/post.cfm>

On the computation of long-range interactions in fluids under confinement: Application to pore systems with various types of spatial periodicity

Evangelia Pantatosaki and George K. Papadopoulos^{a)}

School of Chemical Engineering, National Technical University of Athens, GR 15780 Zografou Campus, Athens, Greece

(Received 1 May 2007; accepted 22 September 2007; published online 31 October 2007)

The problem of computing accurately the long-range Coulomb interactions in physical systems is investigated focusing mainly on the atomistic simulation of fluids sorbed in porous solids. Several articles involving theory and computation of long-range interactions in charged systems are reviewed, in order to explore the possibility of adapting or developing methodology in the field of computer simulation of sorbate molecules inside nanostructures modeled through a three-dimensional (crystal frameworks), two-dimensional (slit-shaped pores), or one-dimensional (cylindrical pores) replication of their unit cell. For this reason we digitally reconstruct selected paradigms of three-dimensional microporous structures which exhibit different spatial periodicities such as the zeolite crystals of MFI and FAU type, graphitic slit-shaped pores, and single-wall carbon nanotubes in order to study the sorption of CO₂, N₂, and H₂ via grand canonical Monte Carlo simulation; the predicted data are compared with experimental measurements found elsewhere. Suitable technical adjustments to the use of conventional Ewald technique, whenever it is possible, prove to be effective in the computation of electrostatic field of all the categories studied in this work. © 2007 American Institute of Physics. [DOI: 10.1063/1.2799986]

I. INTRODUCTION

The accurate calculation of electrostatic forces is of considerable importance for the computer simulation of polar/charged systems subject to periodic conditions. Since the Coulomb potential converges much more slowly than the dispersive short-ranged interactions, the usually employed truncation methods to Lennard-Jones potential cannot apply since long-range-type corrections are diverging. Thus, a sufficient compensation for the missing long-range part of the electrostatic potential field is unfeasible. On the other hand, the obvious alternative of increasing vastly the volume of the simulated system would result in a dramatic increase of the central process unit computation time especially in the case of pore systems where in addition to sorbate-sorbate interactions the electrostatic interactions with the sorbent framework atoms must be taken into account.

As a consequence of the above limitations, computation of electrostatic interactions requires a large number of interacting periodic images of the simulation cell. However, the latter introduces conditional convergence in the evaluated energies as a result of the mixing of signs in the terms of the infinite series involved in the aforementioned potentials. A rigorous way to overcome this problem has been given by Ewald.¹ His method, developed for the evaluation of optical and electrostatic lattice potentials, is a well-established tool for the computation of the electrostatic field in periodic systems consisting of ions or polar molecules.

The work presented in this paper is organized in two main parts. In the first, the mathematical background of the

Ewald method is clarified in a rigorous way akin to its original form¹ in an attempt to reveal the aspects concerning computational studies in nanostructures. Then, a critical literature survey is carried out, aiming at adapting the method to the simulation study of the sorption thermodynamics of polar molecules inside sorbents, bearing charged atoms and being subject to various spatial periodic forms due to their way of modeling. The second part reports our sorption thermodynamics predictions for carbon dioxide, nitrogen, and hydrogen in digitally reconstructed model sorbent systems, which comprise various types of spatial periodicity; the resulted simulated isotherms from this analysis are compared to experimentally measured isotherms found elsewhere.

A. Theory

In many studies pertaining to dynamics and equilibrium of molecules in pore systems as in the present work, it is convenient to represent electrostatic centers by means of partial charges. Derivation of the following equations in the case of dipolar molecules is straightforward and can be found elsewhere.^{2,3}

The classical electrostatic energy for a system of N point charges $\{q_i\}$ located at positions $\{\mathbf{r}_i\}$, $i=1,2,\dots,N$, in a periodically repeated unit cell of volume $V=\mathbf{l}_1\cdot\mathbf{l}_2\times\mathbf{l}_3$, characterized by the set of real space lattice vectors $\{\mathbf{l}_m\}$, $m=1,2,3$, can be written as

$$U = \frac{1}{4\pi\epsilon_0} \frac{1}{2} \sum_{\mathbf{n}} \left(\sum_{i=1}^N \sum_{j=1}^N \frac{q_i q_j}{|\mathbf{r}_{ij} + \mathbf{n}|} \right), \quad (1)$$

where ϵ_0 is the permittivity of vacuum. The prime on the sum indicates that the terms where $|\mathbf{r}_{ij} + \mathbf{n}|=0$ are omitted

^{a)} Author to whom correspondence should be addressed. Electronic mail: gkpap@chemeng.ntua.gr

excluding this way the infinite self-energy of the point charges. The summation over \mathbf{n} is carried out over all integer translations of the real space lattice vectors $\mathbf{n} = n_1\mathbf{l}_1 + n_2\mathbf{l}_2 + n_3\mathbf{l}_3$ for integers n_m , $m = 1, 2, 3$; also, $\mathbf{r}_{ij} \equiv \mathbf{r}_i - \mathbf{r}_j$. Obviously, periodic replication of a non-neutral system toward the calculation of Coulomb interactions via this procedure would be quite meaningless since the sum of Eq. (1) under these conditions diverges.

Nevertheless, the presence of the infinite series $\sum_{\mathbf{n}} |\mathbf{r}_{ij} + \mathbf{n}|^{-1}$ in the above relation makes the sum of Eq. (1) conditionally convergent;⁴ namely, derangement of its terms alters the sum, making any direct attempt to compute Coulomb potential in a neutral infinite system through this formula suffer from lack of a unique value. In the theory of ionic crystals such series of distances between ions known as Madelung constants appear in the calculation of the lattice potential energy. Because calculation of these constants in three dimensions is a vastly complicated procedure,⁵ computation of electrostatic potentials using the formula (1) is by no means a rigorous way for computing long-range interactions in atomistic simulations of periodic systems. An extensive analysis of the conditions of convergence of such series involved in simulation of periodic systems of ions or dipolar molecules can be found in the seminal work of de Leeuw *et al.*^{6,7}

More precisely, introducing the convergence factor $\exp(-s|\mathbf{n}|^2)$ the aforementioned series become $\sum_{\mathbf{n}} |\mathbf{r}_{ij} + \mathbf{n}|^{-1} \exp(-s|\mathbf{n}|^2)$; then they may be forced into absolute convergence by properly converting them to a uniformly convergent series of continuous functions on $s \geq 0$. Subsequently, by virtue of gamma function,⁴ $|\mathbf{r}_{ij} + \mathbf{n}|^{-1}$ is transformed as follows:

$$\begin{aligned} & \sum_{\mathbf{n}} |\mathbf{r}_{ij} + \mathbf{n}|^{-1} \exp(-s|\mathbf{n}|^2) \\ &= \frac{1}{\Gamma(1/2)} \int_0^\infty dt t^{-1/2} \sum_{\mathbf{n}} \exp(-s|\mathbf{n}|^2 - t|\mathbf{r}_{ij} + \mathbf{n}|^2). \quad (2) \end{aligned}$$

Consequently, the problem reduces to the evaluation of the integral in Eq. (2). By splitting this integral into $[0, a^2]$ and $[a^2, \infty]$, and transforming $\exp(-t|\mathbf{r}_{ij} + \mathbf{n}|^2)$ by means of the imaginary transformation of the Jacobi theta functions,⁴ evaluation of the integrals leads to the following lattice sums:⁶

$$\begin{aligned} & \sum_{\mathbf{n}}' |\mathbf{r}_{ij} + \mathbf{n}|^{-1} \exp(-s|\mathbf{n}|^2) \\ &= \sum_{\mathbf{n}}' |\mathbf{r}_{ij} + \mathbf{n}|^{-1} \exp(-s|\mathbf{n}|^2) \operatorname{erfc}(a|\mathbf{r}_{ij} + \mathbf{n}|) \\ &+ \frac{1}{\pi} \sum_{\mathbf{n} \neq 0} |\mathbf{n}|^{-2} \exp(2\pi i \mathbf{n} \cdot \mathbf{r}_{ij} - \pi^2 |\mathbf{n}|^2 / a^2) [1 + o(s)] \\ &- \frac{2\pi}{3} |\mathbf{r}_{ij}|^2 + 2\pi s \sqrt{1 + s/a^2} + o(s). \quad (3) \end{aligned}$$

The parameter a^2 only influences the speed of convergence of the above sums; its physical meaning will be shown in the next paragraph. Also, $\operatorname{erfc}(x)$ is the complementary error

function, defined as $1 - \operatorname{erf}(x)$, where $\operatorname{erf}(x)$ is the error function defined as $2/\sqrt{\pi} \int_0^x \exp(-t^2) dt$.

In the case where vectors, $\mathbf{r}_{ij} + \mathbf{n}$, in the above sums are referred to distances between ions and their own periodic images, then the series under consideration becomes $\sum_{\mathbf{n} \neq 0} |\mathbf{n}|^{-1}$. Therefore, these terms must also be forced into absolute convergence using exactly the same procedure followed above; thus, inserting the resulting expression along with Eq. (3) into Eq. (1), an s -dependent energy expression is established which as $s \rightarrow 0$ it becomes

$$\begin{aligned} U4\pi\epsilon_0 &= \frac{1}{2} \sum_{i=1}^N \sum_{j=1}^N \sum_{\mathbf{n} \neq 0} q_i q_j |\mathbf{r}_{ij} + \mathbf{n}|^{-1} \operatorname{erfc}(a|\mathbf{r}_{ij} + \mathbf{n}|) \\ &+ \frac{1}{2} \left\{ \sum_{\mathbf{n} \neq 0} \left[|\mathbf{n}|^{-1} \operatorname{erfc}(a|\mathbf{n}|) \right. \right. \\ &+ \left. \frac{1}{\pi} |\mathbf{n}|^{-2} \exp(-\pi^2 |\mathbf{n}|^2 / a^2) \right] - \frac{2a}{\sqrt{\pi}} \left. \sum_{i=1}^N q_i^2 \right. \\ &+ \left. \frac{1}{\pi} \sum_{\mathbf{n} \neq 0} q_i q_j |\mathbf{n}|^{-2} \exp(2\pi i \mathbf{n} \cdot \mathbf{r}_{ij} - \pi^2 |\mathbf{n}|^2 / a^2) \right. \\ &+ \left. \frac{2\pi}{3} \left| \sum_{i=1}^N q_i \mathbf{r}_i \right|^2 \right\}, \quad (4) \end{aligned}$$

where the singularity of Eq. (3) at $s=0$ due to terms s^{-1} has now disappeared as a consequence of the vanishing sum, $\sum_{i=1}^N q_i$, contained in these terms because of the charge neutrality of the system.

The magnitude of distance in Eqs. (1)–(4) and the following equations are scaled by a characteristic length, e.g., $|\mathbf{l}_m|$; similarly ϵ_0 is scaled by the same length to have dimensions of $[C^2 J^{-1}]$, so that electrostatic potential U is expressed in Joule.

The method toward the derivation of Eq. (4) uses a mathematical way to arrive at a unique solution to the problem of the computation of electrostatic energy of periodic neutral systems. In addition, since for an electroneutral system the following tautology holds

$$-\frac{1}{2} \sum_{i=1}^N q_i \sum_{j=1}^N q_j |\mathbf{r}_{ij}|^2 = \left| \sum_{i=1}^N q_i \mathbf{r}_i \right|^2,$$

the method does provide a direct explanation of the presence of terms $2\pi/3 |\sum_{i=1}^N q_i \mathbf{r}_i|^2$ [cf. Eqs. (3) and (4)], which represent the total dipole moment of the system. In particular, statistical mechanics correlates the fluctuations of this quantity with polarization effects over the entire volume of the system. Thus, the primary simulation cell polarizes through the spherically repeated periodic images the external surrounding medium of dielectric permittivity ϵ' , which in turn reacts with the simulation cell contributing to the energy U .⁸ de Leeuw *et al.*⁶ have shown that the energy given by the expression (4) corresponds to an ionic system emerged in vacuum ($\epsilon' = 1$), namely, $U \equiv U(\epsilon' = 1)$, the relation of U to the contrary case of a conductor ($\epsilon' \rightarrow \infty$) being

$$U(\epsilon' \rightarrow \infty) = U(\epsilon' = 1) - \frac{2\pi}{3} \left| \sum_{i=1}^N q_i \mathbf{r}_i \right|^2. \quad (5)$$

The assumption of a surrounding of infinite dielectric permittivity employed in the present work by means of combination of Eqs. (4) and (5) involves computation of $U(\epsilon' \rightarrow \infty)$; therefore, an additional physical reason of conditional convergence of Eq. (4) arising from the nature of boundaries at infinity is canceled by removing the term of total dipole moment. Neumann⁹ has reported an extensive study on dipole moment fluctuation formulas for various boundary conditions used in computer simulations of polar systems combining statistical mechanics and electrostatics.

In a less rigorous derivation of Eq. (4), the point charges in the central cell may be replaced by an algebraically equivalent transformation consisting of the N point charges q_i plus N Gaussian charge distributions surrounding and canceling completely each point charge q_i , plus a periodic, usually Gaussian, charge distribution of the same sign with q_i , represented by Fourier series. Subsequently, the electrostatic field due to the aforementioned charge distributions is calculated through Poisson's equation² and the total electrostatic energy $U \equiv U(\epsilon' \rightarrow \infty)$ reads

$$\begin{aligned}
 U4\pi\epsilon_0 = & \frac{1}{2} \sum_{i=1}^N \sum_{j=1}^N \sum_{\mathbf{n}=0}^{\infty} q_i q_j |\mathbf{r}_{ij} + \mathbf{n}|^{-1} \operatorname{erfc}(a|\mathbf{r}_{ij} + \mathbf{n}|) \\
 & + \frac{1}{2} \sum_{i=1}^N \sum_{j=1}^N \sum_{\mathbf{k} \neq 0} q_i q_j \frac{4\pi}{k^2} \exp\left(-\frac{k^2}{4a^2}\right) \cos(\mathbf{k} \cdot \mathbf{r}_{ij}) \\
 & - \frac{a}{\sqrt{\pi}} \sum_{i=1}^N q_i^2. \quad (6)
 \end{aligned}$$

Via the above formulation the real space summation is carried out only in the central simulation cell ($\mathbf{n}=\mathbf{0}$), by suitably adjusting the relative rates of convergence of the real and Fourier space sums by means of value a , whose physical meaning is connected to the second moment s_d of the canceling Gaussian distribution through the formula $a^2=1/2s_d^2$ (see next section). Under these circumstances the second sum with $\mathbf{n} \neq \mathbf{0}$ vanishes; thus, the second term of Eq. (4) simplifies to $-a/\sqrt{\pi} \sum_{i=1}^N q_i^2$. In Eq. (6), this term represents the magnitude to be subtracted at the stage of reciprocal summation, due to the inclusion of the interactions of the periodic Gaussian distributions of charge q_i with the point charge q_i located at the center of this distribution. Instead, one could exclude these interactions directly, as being done at the real space summation, omitting the self-correction term;¹⁰ however, this is usually avoided as it might affect the convergence of the reciprocal part by destroying the periodicity of the Fourier series.

The summation in the reciprocal space is carried out over all integer translations of the vector $\mathbf{k}=2\pi k_1 \mathbf{l}_1^* + 2\pi k_2 \mathbf{l}_2^* + 2\pi k_3 \mathbf{l}_3^*$, for integers k_m , $m=1,2,3$, where the reciprocal lattice vectors $\{\mathbf{l}_m^*\}$ are related to the real space ones by $\mathbf{l}_i \cdot \mathbf{l}_j^* = \delta_{ij}$, where $\delta_{ij}=1$ for $i=j$, and 0 otherwise (Kronecker delta).

Although mathematically efficient, the Ewald summation technique has the inherent disadvantage of being computationally time consuming, since its scaling performance with respect to the number of ions is of $O(N^2)$. Perram *et al.*⁷ showed that an optimal choice of parameters can reduce the

scaling to $O(N^{3/2})$; Fincham¹¹ gave an intuitive proof of Perram's $N^{3/2}$ scaling. Thus, for large systems and especially in the presence of short-range interactions, Ewald method becomes inefficient. This is merely a defect of the Fourier space part, and several algorithms in order to handle this problem in the reciprocal space have been developed.^{12,13}

B. Systems of reduced spatial periodicity

The inhomogeneity introduced by the finite extent in one or two directions of three-dimensional systems prevailing in sorbents, which are modeled by means of primary simulation cells periodically replicated in only two dimensions (e.g., fluids sorbed in slit-shaped pores, adsorption processes on surfaces) or one dimension (e.g., sorption in nanotubes), causes spurious coupling between replicas in this direction.

Heyes *et al.*¹⁴ developed an analytical two-dimensional Ewald-type summation technique for a lamina lattice of singly charged ions, based on the work of Parry¹⁵ and Berthaut,¹⁶ leading to the following expression for the energy:

$$\begin{aligned}
 U4\pi\epsilon_0 = & \frac{1}{2} \sum_{i=1}^N \sum_{j=1}^N \sum_{\mathbf{n}=0}^{\infty} q_i q_j \frac{\operatorname{erfc}(a|\mathbf{r}_{ij} + \mathbf{n}|)}{|\mathbf{r}_{ij} + \mathbf{n}|} \\
 & + \frac{\pi}{2} \sum_{i=1}^N \sum_{j=1}^N \sum_{\mathbf{k} \neq 0} q_i q_j \frac{\cos(\mathbf{k} \cdot \mathbf{r}_{ij})}{k} \times [\exp(kz_{ij}) \operatorname{erfc}(az_{ij} \\
 & + k/2a) + \exp(-kz_{ij}) \operatorname{erfc}(-az_{ij} + k/2a)] \\
 & - \pi \sum_{i=1}^N \sum_{j=1}^N q_i q_j \left[z_{ij} \operatorname{erfc}(az_{ij}) + \frac{1}{a\sqrt{\pi}} \exp(-a^2 z_{ij}^2) \right] \\
 & - \frac{a}{\sqrt{\pi}} \sum_{i=1}^N q_i^2, \quad (7)
 \end{aligned}$$

where $\mathbf{n}=n_1 \mathbf{l}_1 + n_2 \mathbf{l}_2$ and $\mathbf{k}=2\pi k_1 \mathbf{l}_1^* + 2\pi k_2 \mathbf{l}_2^*$, are the two-dimensional (2D) real and reciprocal lattice vectors, respectively; k_m and n_m are integers, $m=1,2$ and z_{ij} is the distance of ions i and j in the z direction. In Eq. (7) the convenient assumption of a conductor surrounding medium was also applied, so that the term involving the total dipole moment vanishes. Smith¹⁷ showed that these terms depend on the summation geometry of the medium under consideration.

Nijboer and de Wette¹⁸ (NW) followed a procedure computing the whole potential in Fourier space with the charged particle distance being separated into an in-plane vector and an out-of-plane constituent, and applied their method to slab shaped lattices of ions. Hautman and Klein¹⁹ (HK) in their study on water molecules confined between two dielectric walls derived a method which also separates the in-plane from the out-of-plane distance between two particles, expressing the short- and long-range contributions to the potential as a Taylor series of the ratio of in-plane and out-of-plane distances; the same system had been studied previously by Rhee *et al.*²⁰ by means of a combination of Ewald summation for the in-plane interaction with explicit multipole summations for the higher order contributions.

A rigorous derivation of equations determining the electrostatic interactions in 2D periodic systems has been pro-

vided by Heyes and van Swol²¹ using the Berthaut¹⁶ method. Lekner²² derived a formula for the sums over Coulomb forces exerted on a charged particle for a bulk system and a system comprising charged particles confined between two parallel walls. The derived sums are rapidly convergent being expressed in terms of trigonometric and Bessel functions; the latter decreases exponentially with z . Later, Grønbech-Jensen *et al.*²³ using the summation techniques of Lekner²² provided a simple way toward a correct evaluation of the self-energies of particles in a partially periodic lattice.

Gzrybowski *et al.*²⁴ applying the Poisson summation formula⁴ on the reciprocal space terms arrived at an expression mathematically equivalent to the 2D analytical Ewald summation result of Eq. (7). Kawata *et al.*²⁵ starting from the 2D analytical summation reduced the computational complexity of the reciprocal part of the potential; the accuracy and efficiency of their method were tested by using a water system in three-dimensional (3D) simulation boxes of various geometries (cube, quadratic prism, and slab) with 2D periodicity. They also proposed a formulation²⁶ for accelerating the calculation of Ewald method in a 2D periodic space by using B -spline interpolations and fast Fourier transforms. Minary *et al.*²⁷ treated directly electrostatic interactions on surfaces, by representing the probability density and the potential in a plane-wave basis.

Comparative studies concerning both the accuracy and computational efficiency of the preceding methods have also been carried out. Widmann *et al.*²⁸ compared the 2D analytical summation,¹⁴ NW, and HK (Ref. 19) and concluded that the HK method is efficient for sufficiently small out-of-plane separations; they also showed that NW method depends significantly on the spatial distributions of the ions. Smith²⁹ proposed the use of a combination of the 2D analytical summation and NW method, in a way that the 2D analytical solution and the NW expression are used at small out-of-plane and large out-of-plane separations, respectively. Jorje *et al.*³⁰ in a Monte Carlo study of water sorbed in nanopores found that the Heyes and van Swol method³¹ is computationally more efficient than the 2D analytical solution. Also, the approximation introduced by Rhee *et al.*²⁰ tends to be less accurate at large out-of-plane separations, contrary to the Lekner approach²² which needs a prohibitively large number of terms in the summation in order to overcome the poor divergence for small out-of-plane separations.

Liem *et al.*³¹ implementing the Lekner method²² compared the accuracy of the potential and the forces derived from the 2D analytical formula and the HK method;¹⁹ they showed that the analytical solution is more efficient than, the HK and not depending on charge distribution. Mazars³² compared Lekner's method²² with the work of Parry¹⁵ on a bilayer Wigner crystal of evenly distributed point ions and found both methods to be in close agreement.

An alternative way to compute the long-range interactions in periodic systems with finite periodicity in one dimension is to use the 3D Ewald summation by replicating the finite direction with the inclusion of a sufficiently large vacuum space. Shelley and Pattey³³ used this approach to simulate water confined between planar hydrophobic walls. Spohr,³⁴ simulating water molecules supported by a simple

model surface, showed that the potential function obtained by this procedure converges to the one obtained by Eq. (3) as the simulation box size along the finite direction increases.

Holm *et al.*^{35,36} applied an electrostatic layer correction term to increase the efficiency of the calculation for the contributions of the image layers in 3D replicated slab systems. Bródka³⁷ derived a new theoretical expression for the cutoff error in the 2D reciprocal space summation due to correction term of Holm *et al.*^{35,36} and subsequently used it to determine the optimal height of the simulation box including the vacuum.

An alternative to Ewald technique for one-dimensional (1D) periodic systems due to Boda *et al.*³⁸ introduces the charge line method to compute Coulombic interactions inside a cylindrical pore. Their technique may suffer from singularity problems when the edge of the image line overlaps with an ion in the central cylinder. Tang *et al.*³⁹ showed that the charge line method can be improved by replacing the first section of the image charge line with an image point.

Porto,⁴⁰ through the Γ function using the Poisson summation formula, developed an analogous to Ewald technique for 1D periodic systems.

Bródka⁴¹ gave also an Ewald-type expression for 1D periodic systems both for ionic and dipole interactions leading to the same result obtained by Porto⁴⁰ for the real space sum. Then, he separated the reciprocal sum for $k_z=0$ and $k_z \neq 0$; the first case led to the same result found in Ref. 40 whereas the latter part took a simpler expression.

II. SIMULATION DETAILS

The simulated sorption experiments of gases in the sorbate systems studied in this work were performed by employing a grand canonical Monte Carlo sampling in order to calculate phase space averages.^{3,4,42} In particular, the version of algorithm due to Adams adopted here involves the quantity B which is related to the excess chemical potential μ^{ex} of the sorbed phase inside the pore volume V at temperature T through the relation:

$$B = \frac{1}{k_B T} \mu^{\text{ex}} + \ln \langle N \rangle_{\mu VT}. \quad (8)$$

B is related to fugacity f of the bulk phase being in equilibrium with the sorbed phase according to equation

$$Vf = k_B T \exp(B), \quad (9)$$

where k_B is the Boltzmann constant. In the remainder of this work fugacity approximates to pressure assuming that bulk phase behaves ideally.

The diatomic N_2 molecule was modeled as a dumbbell with a rigid interatomic bond of 0.1098 nm length.⁴³ The triatomic linear molecule of CO_2 was modeled as two consecutive dumbbells sharing the central C atom, arranged on a straight line, with C–O length of 0.1149 nm.⁴⁴ To describe the interactions, a simplified representation was used, cast in terms of Lennard-Jones sites on the atoms and partial charges on the molecular axis. Partial charges were distributed around each molecule so as to reproduce experimental quadrupole moments (see Ref. 45 and references therein).

TABLE I. Lennard-Jones parameters for the sorbate molecules and sorbent atoms.

	ϵ/k_B (K)	σ (nm)
C–C	28.129	0.2757
O–O	80.507	0.3033
N–N	36.4	0.3318
O ^a –O ^a	89.6	0.2806
C ^b –C ^b	772.0	0.253
Na–Na	80.0	0.320
H ₂ –H ₂	36.5	0.282
H ₂ –O ^a	40.0	0.383
H ₂ –Na	34.0	0.380

^aZeolite oxygen.^bCarbon model pores.

The molecule of H₂ was modeled as one Lennard-Jones site bearing a weak quadrupole moment across a bond length of 0.0741 nm.⁴⁶ The parameters of H₂ presented in Table I resulted from calibration with respect to bulk experimental data found in the work of Kumar *et al.*⁴⁷ (see next section). All the strength and size parameters as well as the values of partial charges of the sorbates used in the present study are presented in Tables I and II.

For the short-ranged sorbate-sorbate and sorbate-zeolite atom interactions, the Lennard-Jones potential was used, i.e.,

$$U(r_{ij}) = 4\epsilon_{ij} \left[\left(\frac{\sigma_{ij}}{r_{ij}} \right)^{12} - \left(\frac{\sigma_{ij}}{r_{ij}} \right)^6 \right]. \quad (10)$$

For the hydrogen molecule, the approximation due to Feynman-Hibbs⁴⁸ was employed for all the involved dispersion-type interactions in order to account for its quantum nature, i.e.,

$$U_{\text{FH}}(r_{ij}) = U_{\text{LJ}}(r_{ij}) + \frac{\hbar^2}{24m_r k_B T} \left[\frac{\partial^2 U_{\text{LJ}}(r_{ij})}{\partial r_{ij}^2} + \frac{2}{r_{ij}} \frac{\partial U_{\text{LJ}}(r_{ij})}{\partial r_{ij}} \right], \quad (11)$$

where m_r is the reduced mass of the interacting pair given by $m_r^{-1} = M_i^{-1} + M_j^{-1}$; M denotes molecular mass and subscripts specify the pair interaction type, e.g., H₂–H₂ ($i=j$) or H₂

TABLE II. Partial charges.

	q (e)
CO ₂	–0.325 6 (O)
	+0.651 2 (C)
N ₂	–0.404 84 (N)
	+0.809 68 (center of mass)
H ₂	+0.482 9 (H)
	–0.965 8 (center of mass)
Si	+2.000 (silicalite 1, DAY)
	+2.050 (NaY, NaX)
Al	+1.750
O	–1.000 (silicalite, DAY)
O _{Si}	–1.025 (NaY, NaX) ^a
O _{Al}	–1.200 (NaY, NaX) ^b
Na	+1.000

^aFramework oxygen bonded with two Si atoms.^bFramework oxygen bonded with one Si and one Al atom.TABLE III. Box lengths and \mathbf{k} vectors used for the 3D approximation of the Ewald summation to pore systems with 2D spatial periodicity.

$l_1=l_2$ (nm)	l_3 (nm)	$k_1=k_2$	k_3
10	0.65	8	2
10	0.95	8	4
10	1.45	8	5
10	2.15	8	7

with any atom in the zeolite framework ($i \neq j$).

Since the sorbate molecules we studied bear more than one charged centers ($m \neq 1$), the following term

$$U_{\text{intra}} = \sum_i^N \sum_{k=1}^m \sum_{l>k}^m \frac{q_k q_l \text{erf}(a|\mathbf{r}_{kl}|)}{|\mathbf{r}_{kl}|}, \quad (12)$$

needed to be subtracted from the total potential electrostatic energy since it represents the intramolecular energy between point charges located at positions $\mathbf{r}_1, \mathbf{r}_2, \dots, \mathbf{r}_m$ on the same molecule, due to interaction of each of them with the periodic Gaussian distributions surrounding every neighbor at distance $|\mathbf{r}_{kl}|$. The reason is that these interactions have been included in the computation of the reciprocal part as we did for the self-term discussed above.

The value of a in the equations of electrostatic energy, as mentioned in the preceding section, controls the relative rate of convergence of the sums appeared in them, reflecting the interplay between the convergence rate of real and reciprocal sums. Therefore, high values of a accelerate the real summation part, making at the same time k -space part require a higher number of vectors to converge and vice versa; in any case the reciprocal sum is the expensive computational task.

In order to diminish the computational efforts concerning both the short- and long-range sorbate-sorbent interactions, when sorbent is modeled as a nonflexible framework of atoms such as the zeolite crystals of this work, we mapped these interactions prior to actual simulation run, with the sorbate-sorbate interactions being computed interactively (see next section).

The amorphous model graphitic substrates and nanotubes are modeled with no charges on their atoms. For the sorbate-sorbate interactions in the carbon slits the technique of Shelley and Pattey³³ was followed; in model nanotubes, Eq. (1) proved to be adequate approximation when applied in a long simulation box (400–500 nm). For all the systems of this study the total number of particles varied between 600 and 800 particles to ensure good statistics; especially in the high pressure regime of the predicted isotherms.

The k_m values used in the carbon slit model for several sizes of pore widths l_3 are listed in Table III, a value of the dimension bounding the empty space, in the range of three to five times the pore width was adequate for sufficient convergence. With this choice of parameters, the value of the reciprocal space sum was proved to have negligible effect to the total electrostatic energy being thus practically determined by the real space sum. Negligible contributions of the recip-

rocal space sum have also been reported by Rycerz and Jacobs⁴⁹ in molecular dynamics simulations of Bi₂O₃ and of a crystalline and molten NaCl system.

III. RESULTS AND DISCUSSION

A. Digital reconstruction of sorbents

Graphite-based materials belong to a popular category of amorphous microporous sorbents mostly in the form of carbon membranes and lately of nanotubes. The slit-shaped carbon pores in this work were modeled as close packed layers of noncharged carbon atoms, according to the procedure described in Ref. 50. The adsorbent was constructed as layers made up from close packed carbon atoms to represent an elementary unit of a graphitic material with parameters ϵ_{ss} and σ_{ss} , and separated by distance $z_0 = 2^{1/6}\sigma_{ss}$. To obtain cylindrical nanopores, the graphite layers were wrapped into an annulus with the potential parameters of the model being calibrated with respect to real carbon materials.⁵⁰

Zeolites constitute nanoporous crystalline aluminosilicate frameworks, wherein Si and Al atoms (T atoms) are bonded via O atoms in such a way that bonds of the type Al–O–Al are excluded (Löwenstein's rule⁵¹); depending on the Si/Al ratio, they may contain extraframework cations, so that the negative charge of Al atoms can be compensated.⁵²

The procedure we followed for reconstructing a digital crystal entails the following: (i) finding from Ref. 53 the unit cell geometric characteristics that correspond to the particular framework type code, and then from the x-ray-diffraction (XRD) spectrum in the same reference, or neutron diffraction data found elsewhere (see below) locating the position vectors of the "primary" framework atoms; (ii) applying the symmetry operations of the relevant space group the crystal belongs to, which are given in Ref. 54. The types and position vectors of all framework and off-framework atoms of the unit cell, taking into account their occupancy probability found from the XRD analysis or neutron diffraction data, are finally generated to form a computer model of the unit cell. Because the Al and Si atoms are indistinguishable by the XRD technique, in several positions the occupation probability is less than unity.⁵³

According to the above procedure the MFI-type silicalite-1 crystal (Si₁₉₂O₃₈₄) was modeled in its orthorhombic form (*Pnma* space group) forming a rigid framework according to x-ray diffraction crystallographic data⁵⁵ following the symmetry operations of the space group; the lattice parameters of the unit cell are $a=2.007$ nm, $b=1.992$ nm, and $c=1.342$ nm.

For the FAU-type crystal of purely siliceous DAY (Si₁₉₂O₃₈₄), a similar to silicalite procedure was followed utilizing powder neutron diffraction data⁵⁶ and the symmetry operations of the *Fd $\bar{3}m$* space group (cubic symmetry), its lattice parameter being 2.425 76 nm. For the charged NaY (Na₅₆Al₅₆Si₁₃₆O₃₈₄) and NaX (Na₈₆Al₈₆Si₁₀₆O₃₈₄) FAU crystals, we used as input spectra from powder neutron diffraction⁵⁷ and x-ray diffraction⁵⁸ employing the proper operations under *Fd $\bar{3}m$* and *Fd $\bar{3}$* space groups, respectively, their lattice parameters being, respectively, 2.485 36 and 2.5099 nm.

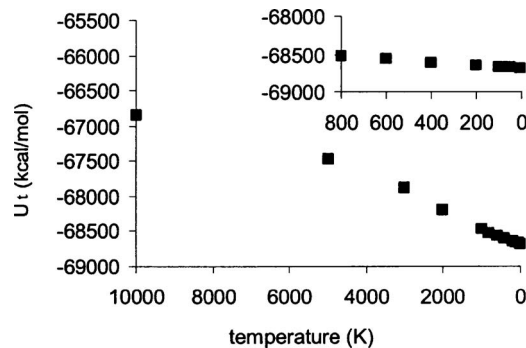


FIG. 1. Total energy plateau during the simulated annealing minimization procedure in NaY; the last runs locating the minimum global energy of the crystal are depicted in the inset.

The Si/Al ratio in the framework of charged zeolites not only determines the anionic charge per unit cell and thereby the number of cations but also affects the distribution of cations among the various kinds of sites present in the unit cell; the notation for the topology of these sites and their occupancy by monovalent sodium can be found in the monograph of Barrer.⁵² In the framework of NaY the crystallographic site II was considered completely occupied and sites I' and I partially occupied by Na⁺.⁵⁷ In NaX the sites II and I' were considered completely occupied by Na⁺ and the remainder cations were distributed to site III.⁵⁹ A convenient way of modeling the partial charge distribution in the framework is to give T atoms an average partial charge, depending on the particular Si/Al ratio.⁶⁰ However, it is an oversimplification, since it does not take into account the different polarizations of oxygens bonded to Si or Al atoms.

In this study we used the model of Jaramillo and Auerbach⁶¹ which explicitly distinguishes the Si and Al atoms attributing different partial charges for the oxygen framework atoms, according to the neighboring bonded T atoms. For this reason we randomly distributed T atoms in the framework up to the desired ratio Si/Al in such a way that Löwenstein's rule is fulfilled. In addition, the energy of the crystal was minimized by means of simulated annealing technique⁶² before the actual grand canonical Monte Carlo runs (Fig. 1). The resulted difference in the positions of cations from the ones used in Ref. 58 over the range of temperatures used was negligible.

In zeolite crystals, modeled as rigid in this work, electrostatic fields were computed on a three-dimensional grid of

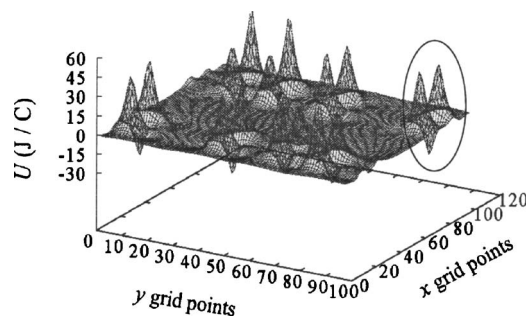


FIG. 2. Computed electrostatic field contour for silicalite 1 at $z=0$ nm; the circled region denotes the part of the field due to asymmetric unit.

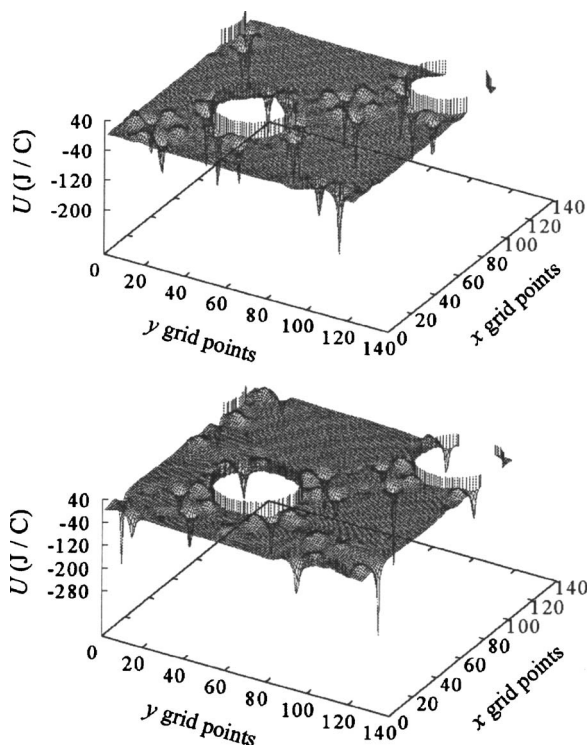


FIG. 3. Indicative computed electrostatic field contours for dealuminated Y (DAY) (top) and NaX (bottom) faujasites, at $z=2.27$ nm denoting the subtracted sodalite interiors.

0.2 Å spacing over the unit cell. The field of silicalite 1 was pretabulated over the asymmetric unit, namely, the 1/8 of its unit cell volume to save computational time (Fig. 2); then, by virtue of the symmetry operations carried out in the orthorhombic form of silicalite crystal, computation of the field was extended at any point in the simulation cell during run time. This procedure was first followed by June *et al.* for the Lennard-Jones potential.⁶³ An example of computed electrostatic energy contours is illustrated in Fig. 2. Sorbate-zeolite interactions were pretabulated and the values at any certain point in the unit cell were estimated by means of a fast 3D Hermite interpolation scheme⁶⁴ during the actual simulation run. This strategy reduces significantly the CPU time for the Ewald sums, therefore, allows efficient phase space sampling by including a larger number of unit cells in the simulation box.

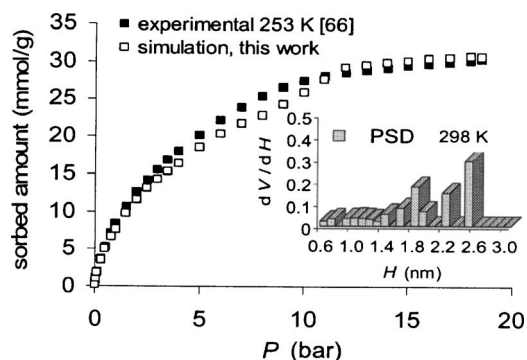


FIG. 4. Experimental (filled symbols) and predicted sorption isotherms for carbon slits (open symbols) based on the computed PSD (inset), for CO₂ in AX-21.

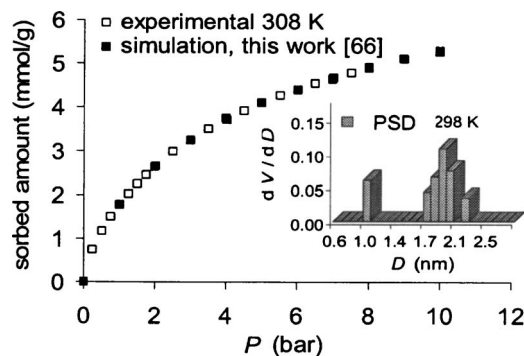


FIG. 5. Experimental (filled symbols) and predicted sorption isotherms for carbon nanotubes (open symbols) based on the computed PSD (inset) for CO₂ in Norit RB4.

Moreover, we used tabulation of the electrostatic potential in order to make selected areas of the crystal framework inaccessible to sorbate host molecules by artificially excluding these areas from the phase space sampled by grand canonical Monte Carlo algorithm. In particular, this way, we eliminated the interior of sodalite cages in faujasite crystals (Fig. 3) in order to exclude this space from the modeled system since the sizes of CO₂, N₂, and H₂ molecules do not physically permit entrance to these areas.

The positions of cations in the charged FAU-type zeolites of the present work remained unchanged during the simulation. Calero *et al.*⁶⁵ showed that this assumption is valid for the modeling of sorption even for much longer sorbate molecules such as *n*-alkanes.

B. Sorption isotherms

CO₂/carbon materials. For slit-shaped micropores, the sample used is the typical activated carbon material, AX21.

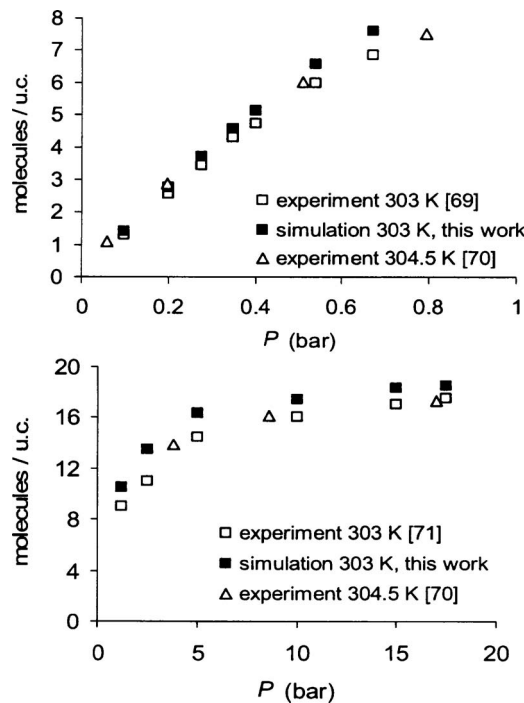
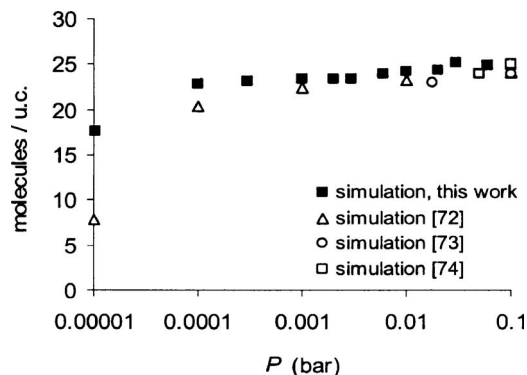


FIG. 6. Low (top) and higher (bottom) pressure sorption isotherms of CO₂ in silicalite 1.

FIG. 7. Sorption isotherms of N_2 in silicalite 1 at 77 K.

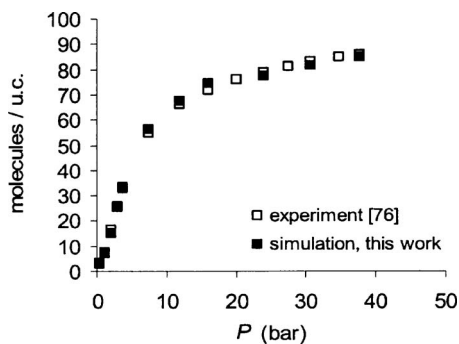
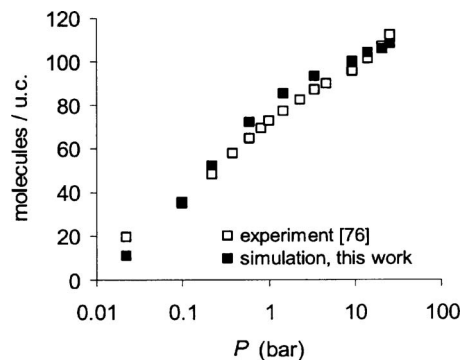
For cylindrical micropores, the sample is a commercially available activated carbon, Norit RB4.⁶⁶ Since amorphous carbon materials consist of no unique pores, a way of weighting the calculated density of sorbates in individual models of various sizes must be found in order to capture the morphology of the real sorbent. For this reason we computed a pore size distribution (PSD) by numerically analyzing the simulated data in a series of individual model units of several pore sizes, with respect to measured data of a real carbon material under exactly similar conditions.^{66,67} A successfully predicted PSD then (insets in Figs. 4 and 5), in conjunction with simulated data at any temperature, can generate the sorption isotherm at this temperature.

The CO_2 isotherms inside the carbon slits at 298 K under various pressures and several pore widths were computed using the method of Shelley and Pattey³³ for the long-range interactions, suitably adapted for the system of this work (see Table III).

Figure 4 shows the successful comparison of the predicted isotherms of CO_2 in the carbon slit-shaped pores with the measured ones in AX21 over a wide range of pressure values up to saturation loadings.

In Fig. 5 the results of the predicted isotherm in model carbon nanotubes combined with the PSD extracted from Norit RB4 are seen to be in good agreement with the experimental data in the same material.

CO_2 , N_2 /silicalite 1. The CO_2 and N_2 sorption isotherms in silicalite 1 were computed using the technique discussed in the preceding section in order to calculate the long-range interactions. Regarding the dispersive interactions with zeo-

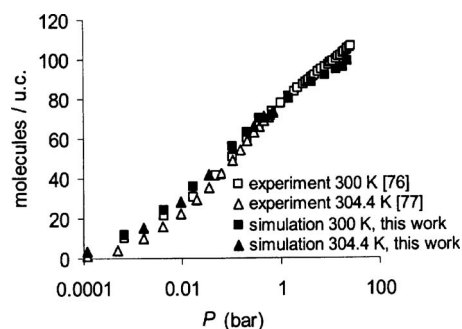
FIG. 8. Sorption isotherms of CO_2 in dealuminated Y faujasite (DAY) at 300 K.FIG. 9. Sorption isotherms of CO_2 in $Na_{56}Y$ at 300 K.

lite atoms, T atoms were excluded, following the approach of Kiselev *et al.*⁶⁸ The Lennard-Jones parameters used in simulations are presented in Table I. A comparison between our computed and measured experimentally isotherms found in Refs. 69–71 is shown in Fig. 6; the data points are in good agreement over a wide range of loadings starting from Henry's law regime (top) up to saturation (bottom).

The N_2 sorption predictions for pressures greater than 10^{-4} bar are satisfactorily compared with the experimental data of Mueller *et al.*,⁷² Song *et al.*,⁷³ and Llewellyn *et al.*,⁷⁴ as illustrated in Fig. 7. Below this pressure the model overpredicts the experimental data. This obviously indicates that the Lorentz-Berthelot combining rules³ used to calculate the cross interaction parameters are not adequate to model sorption thermodynamics at Henry's law region wherein sorbate-sorbent interactions are dominant.

Previous extensive simulation studies⁴⁵ of the two aforementioned systems carried out for various sorbate molecule models on the three symmetries of the silicalite crystal involved Eq. (1) for high values of vector \mathbf{n} (up to 30 000 unit cells) toward the mapping of the electrostatic interactions with the zeolite atoms. Their results from this simple summation scheme show no significant difference in the sorption of carbon dioxide, whereas in the case of nitrogen, the inclusion of Ewald-type calculations of this work leads to a better agreement with experimental results and explains noticeable effects observed experimentally near saturation.⁷⁵

CO_2 /DAY, NaX, NaY. The CO_2 sorption isotherm in DAY at 300 K for various pressures up to 40 bars is shown in Fig. 8. The electrostatic energy was computed using the same partial charges for the framework atoms, Si and O, and Lennard-Jones parameters for O, which we used in silicalite

FIG. 10. Sorption isotherms of CO_2 in $Na_{86}X$ at 300 and 304.4 K.

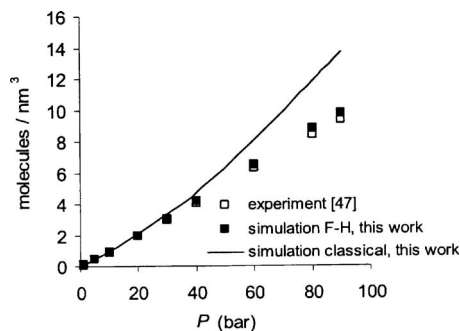


FIG. 11. Experimental and simulated isotherms using conventional and quantum mechanically corrected (Ref. 48) Lennard-Jones potential of bulk hydrogen at 77 K.

1, since DAY is the siliceous (dealuminated) analog of faujasite. In Fig. 8 also a comparison with the measured isotherm due to Maurin *et al.*⁷⁶ is presented.

The CO₂ sorption isotherms in NaY and NaX computed at 300 and 304.4 K are shown in Figs. 9 and 10. The dispersion energy part was calculated using the same parameters for the framework atoms of DAY. The Lennard-Jones interaction parameters of sodium cations (Table I) were calibrated with respect to experimental data.^{76,77}

H₂/NaX. The short-ranged potential parameters of H₂-H₂, as already discussed resulted from calibration with respect to bulk H₂ density data at 77 K found in the work of Kumar *et al.*;⁴⁷ it must be noticed that the hydrogen molecule in their work was modeled as neutral sphere.

In this work, use of Feynman-Hibbs potential up to the second order term led to a higher value for ϵ/k_B and a slightly lower value for σ compared to the parameters reported by Buch⁷⁸ (34.2 K and 0.296 nm, respectively). Our predicted isotherm of bulk H₂ versus the experimental points is shown in Fig. 11. As can be seen from the same graph, the classical treatment by means of the conventional Lennard-Jones potential is not adequate to represent the short-ranged interactions especially as the bulk becomes denser.

In Fig. 12 is shown the computed H₂ sorption isotherm in NaX at 77 K. It must be noticed that in this graph the cross Lennard-Jones parameters for hydrogen-zeolite oxygen atoms and hydrogen-sodium cations interactions (see Table I) needed calibration with respect to the experimental data shown in the same graph in order to match the measured

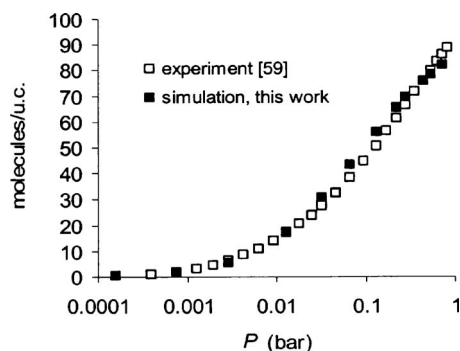


FIG. 12. Experimental and predicted sorption isotherms of H₂ in Na₈₆X at 77 K using the approach of Feynman-Hibbs (Ref. 48) for the description of all types of dispersive interactions.

points at higher loadings. This deviation reflects the inadequacy of the hydrogen state inside the porous material being described by the bulk phase energetics. More sophisticated quantum approaches for the hydrogen molecules inside the sorbent space would certainly offer a more adequate description than the one provided by the magnitude of quantum effect through Eq. (11). Such a treatment remains out of the scope of this work and can be found elsewhere.^{79,80}

IV. CONCLUSIONS

In this work we investigated the problem of computing accurately the long-range Coulombic interactions in physical systems, and then focusing on the atomistic simulation of fluids sorbed in porous solids, we studied the calculation of the electrostatic field in three-dimensional pore structures which may exhibit various types of spatial periodicity. In an attempt to clarify the mathematical background of the Ewald technique we appealed to transcendental functions through properly selected convergence factors, adopting the rigorous methodology of de Leeuw *et al.*⁶

We reviewed various articles involving theory and computation of long-range interactions in ionic and polar systems, aiming at the investigation of the possibility of adapting or developing methodology in the atomistic computer simulation of sorbate molecules bearing partial charges, inside microstructures modeled through a three-, two-, or one-dimensional replication of their unit cell.

We reconstructed the carbon materials via computed pore size distributions extracted from experimental data under the same conditions with simulation, whereas the crystal structure of zeolites allowed a digital representation in atomistic level by virtue of spectra and symmetry operations known from crystallographic data. Subsequently, we studied the sorption thermodynamics of carbon dioxide, nitrogen, and hydrogen via grand canonical Monte Carlo simulation in parallel with experimental measurements in the aforementioned nanopore models in order to investigate the effect of the modeling parameters on the computer simulation of molecules under confinement. The conclusion drawn from the study in the crystals of faujasite and silicalite proved that application of the conventional Ewald summation method by precomputing the interactions in the form of a pretabulated map of the electrostatic potential field is an efficient way to overcome the time consuming explicit calculations of the reciprocal space. On the other hand, it allows inclusion of a higher number of crystals in the primary simulation box so that a better statistics is attained. The work on the graphitic microporous media revealed the advantage of employing the conventional Ewald technique in a system involving slabs of vacuum along its nonperiodic direction by suitable parametrization of the real and reciprocal space parts. For the model carbon nanotubes we used the simple expression for Coulombic interactions summing over an elongated primary simulation box. These choices are strongly supported from the fact of the high computational efforts required for the analytical Ewald-type summations.

ACKNOWLEDGMENTS

We are grateful to Dr. Hervé Jobic for providing us with the experimental measurements of hydrogen in NaX. Support by the European Union via the FP6-Marie Curie research training network (MRTN-CT-2004-005503) is acknowledged.

- ¹ P. Ewald, *Ann. Phys.* **64**, 253 (1921).
- ² D. Frenkel and B. Smit, *Understanding Molecular Simulation: From Algorithms to Applications* (Academic, London, 2002).
- ³ M. P. Allen and D. J. Tildesley, *Computer Simulation of Liquids* (Clarendon, Oxford, 1987).
- ⁴ E. T. Whittaker and G. N. Watson, *A Course of Modern Analysis* (Cambridge University Press, Cambridge, 2000).
- ⁵ M. Born and K. Huang, *Dynamical Theory of Crystal Lattices* (Oxford University Press, Oxford, 1954).
- ⁶ S. W. de Leeuw, J. W. Perram, and E. R. Smith, *Proc. R. Soc. London, Ser. A* **373**, 27 (1980).
- ⁷ J. W. Perram, H. G. Peterson, and S. W. de Leeuw, *Mol. Phys.* **65**, 875 (1988).
- ⁸ L. Onsager, *J. Am. Chem. Soc.* **58**, 1486 (1936).
- ⁹ M. Neumann, *Mol. Phys.* **50**, 841 (1983).
- ¹⁰ R. Snurr, <http://www.chem-biol-eng.northwestern.edu/people/faculty/snurr.html>
- ¹¹ D. Fincham, *Mol. Simul.* **3**, 1 (1994).
- ¹² J. W. Eastwood and R. W. Hockney, *J. Comput. Phys.* **16**, 342 (1974).
- ¹³ U. Essmann, L. Perera, M. L. Berkowitz, T. Darden, H. Lee, and L. G. Pedersen, *J. Chem. Phys.* **103**, 8577 (1995).
- ¹⁴ D. M. Heyes, M. Barber, and J. H. R. Clarke, *J. Chem. Soc., Faraday Trans. 2* **73**, 1485 (1977).
- ¹⁵ D. E. Parry, *Surf. Sci.* **49**, 433 (1975).
- ¹⁶ E. F. Berthaut, *J. Phys. Radium* **13**, 499 (1952).
- ¹⁷ E. R. Smith, *Mol. Phys.* **65**, 1089 (1988).
- ¹⁸ B. R. A. Nijboer and F. W. de Wette, *Physica (Amsterdam)* **23**, 309 (1957); B. R. A. Nijboer, *Physica A* **125**, 275 (1984).
- ¹⁹ J. Hautman and M. L. Klein, *Mol. Phys.* **75**, 379 (1992).
- ²⁰ Y.-J. Rhee, J. W. Halley, J. Hautman, and A. Rahman, *Phys. Rev. B* **40**, 36 (1989).
- ²¹ D. M. Heyes and F. van Swol, *J. Chem. Phys.* **75**, 5051 (1981).
- ²² J. Lekner, *Physica A* **176**, 485 (1991).
- ²³ N. Grønbech-Jensen, G. Hummer, and K. M. Beardmore, *Mol. Phys.* **92**, 941 (1997).
- ²⁴ A. Gzrybowski, E. Gwozdz, and A. Brodka, *Phys. Rev. B* **61**, 6706 (2000).
- ²⁵ M. Kawata and M. Mikami, *Chem. Phys. Lett.* **340**, 157 (2001).
- ²⁶ M. Kawata, M. Masuhiro, and U. Nagashima, *J. Chem. Phys.* **116**, 3430 (2002).
- ²⁷ P. Minary, M. E. Tuckerman, K. A. Pihakari, and G. J. Martyna, *J. Chem. Phys.* **116**, 5351 (2002).
- ²⁸ A. H. Widmann and D. B. Adolf, *Comput. Phys. Commun.* **107**, 167 (1997).
- ²⁹ E. R. Smith, *Proc. R. Soc. London, Ser. A* **375**, 475 (1981).
- ³⁰ M. Jorje and N. A. Seaton, *Mol. Phys.* **100**, 2017 (2002).
- ³¹ S. Y. Liem and J. H. R. Clarke, *Mol. Phys.* **92**, 19 (1997).
- ³² M. Mazaars, *Mol. Phys.* **103**, 1241 (2005).
- ³³ J. C. Shelley and G. N. Pattey, *Mol. Phys.* **88**, 385 (1996).
- ³⁴ E. Spohr, *J. Chem. Phys.* **107**, 16 (1997).
- ³⁵ A. Arnold, J. de Joannis, and Ch. Holm, *J. Chem. Phys.* **117**, 2496 (2002).
- ³⁶ J. de Joannis, A. Arnold, and Ch. Holm, *J. Chem. Phys.* **117**, 2503 (2002).
- ³⁷ A. Bródka, *Chem. Phys. Lett.* **410**, 446 (2005).
- ³⁸ D. Boda, D. D. Busath, D. Henderson, and S. Sokolowski, *J. Phys. Chem. B* **104**, 8903 (2000).
- ³⁹ Y. W. Tang and K. Y. Chan, *Mol. Simul.* **30**, 63 (2004).
- ⁴⁰ M. Porto, *J. Phys. A* **33**, 6211 (2000).
- ⁴¹ A. Bródka, *Chem. Phys. Lett.* **363**, 604 (2002).
- ⁴² J.-M. Leyssale, G. K. Papadopoulos, and D. N. Theodorou, *J. Phys. Chem. B* **110**, 22742 (2006).
- ⁴³ C. S. Murthy, K. Singer, M. L. Klein, and I. R. McDonald, *Mol. Phys.* **41**, 1387 (1980).
- ⁴⁴ J. G. Harris and K. H. Jung, *J. Phys. Chem.* **99**, 12021 (1995).
- ⁴⁵ K. Makrodimitris, G. K. Papadopoulos, and D. N. Theodorou, *J. Phys. Chem. B* **105**, 777 (2001).
- ⁴⁶ D. Marx and P. Nielaba, *Phys. Rev. A* **45**, 8968 (1992).
- ⁴⁷ A. V. A. Kumar, H. Jobic, and S. K. Bhatia, *J. Phys. Chem. B* **110**, 16666 (2006).
- ⁴⁸ R. P. Feynman and A. R. Hibbs, *Quantum Mechanics and Path Integrals* (McGraw-Hill, New York, 1965).
- ⁴⁹ Z. Rycerz and P. Jacobs, *Mol. Simul.* **8**, 197 (1992).
- ⁵⁰ G. K. Papadopoulos, D. Nicholson, and S.-H. Suh, *Mol. Simul.* **22**, 237 (1999).
- ⁵¹ W. Lowenstein, *Am. Mineral.* **39**, 92 (1954).
- ⁵² R. M. Barrer, *Zeolites and Clay Minerals as Sorbents and Molecular Sieves* (Academic, London, 1978).
- ⁵³ Ch. Baerlocher, W. M. Meier, and D. H. Olson, *Atlas of Zeolite Framework Types*, 5th ed. (Elsevier, Amsterdam, 2001).
- ⁵⁴ *International Tables for Crystallography*, 5th ed., Space-Group Symmetry Vol. A, edited by C. T. Hahn (Kluwer Academic, Norwell, MA, 2002).
- ⁵⁵ D. H. Olson, G. T. Kokotailo, S. L. Lawton, and W. M. Meier, *J. Phys. Chem.* **85**, 2238 (1981).
- ⁵⁶ J. J. Hrijac, M. M. Eddy, A. K. Cheetham, J. A. Donohue, and G. J. Ray, *J. Solid State Chem.* **106**, 66 (1993).
- ⁵⁷ A. N. Fitch, H. Jobic, and A. Renouprez, *J. Phys. Chem.* **90**, 1311 (1986).
- ⁵⁸ D. H. Olson, *Zeolites* **15**, 439 (1995).
- ⁵⁹ H. Jobic (private communication).
- ⁶⁰ E. S. M. Auerbach, L. M. Bull, N. J. Henson, H. I. Metiu, and A. K. Cheetham, *J. Phys. Chem.* **100**, 5923 (1996).
- ⁶¹ D. E. Jaramillo and S. M. Auerbach, *J. Phys. Chem. B* **103**, 9589 (1999).
- ⁶² S. Kirkpatrick, C. D. Gelatt, Jr., and M. P. Vecchi, *Science* **220**, 671 (1983).
- ⁶³ R. L. June, A. T. Bell, and D. N. Theodorou, *J. Phys. Chem.* **94**, 1508 (1990).
- ⁶⁴ M. H. Schultz, *Spline Analysis* (Prentice-Hall, New York, 1972).
- ⁶⁵ S. Calero, D. Dubbeldam, R. Krishna, B. Smit, T. Vlucht, J. Denayer, J. Martens, and T. Maesen, *J. Am. Chem. Soc.* **126**, 11377 (2004).
- ⁶⁶ E. Pantatosaki, D. Psomadopoulos, Th. Steriotis, A. K. Stubos, A. Papaioannou, and G. K. Papadopoulos, *Colloids Surf., A* **241**, 127 (2004).
- ⁶⁷ E. Pantatosaki, A. Papaioannou, A. K. Stubos, and G. K. Papadopoulos, *Appl. Surf. Sci.* **253**, 5606 (2007).
- ⁶⁸ A. V. Kiselev, A. A. Lopatkin, and A. A. Shulga, *Zeolites* **5**, 261 (1985).
- ⁶⁹ T. Yamazaki, K. Masahiro, O. Sentaro, and O. Yoshisada, *Mol. Phys.* **80**, 313 (1993).
- ⁷⁰ T. C. Golden and S. Sicar, *J. Colloid Interface Sci.* **162**, 182 (1994).
- ⁷¹ A. Hirotoni, K. Mizukami, R. Miura, H. Takaba, T. Miya, A. Fahmi, A. Stirling, M. Kubo, and A. Miyamoto, *Appl. Surf. Sci.* **120**, 81 (1997).
- ⁷² U. Mueller, H. Reichert, E. Robens, K. K. Unger, Y. Grillet, F. Rouquerol, J. Rouquerol, P. Donfeng, and A. Mersmann, *Fresenius' Z. Anal. Chem.* **333**, 433 (1989).
- ⁷³ L. Song, Z. Sun, L. Duan, S. Jiang, and L. V. C. Rees, *Stud. Surf. Sci. Catal.* **154**, 1797 (2004).
- ⁷⁴ P. L. Llewellyn, J.-P. Coulomb, Y. Grillet, J. Patarin, G. Andre, and J. Rouquerol, *Langmuir* **9**, 1852 (1993).
- ⁷⁵ E. Pantatosaki *et al.* (unpublished).
- ⁷⁶ G. Maurin, P. L. Llewellyn, and R. G. Bell, *J. Phys. Chem. B* **109**, 16084 (2005).
- ⁷⁷ J. A. Dunne, R. Mariwals, M. Rao, S. Sircar, R. J. Gorte, and A. L. Myers, *Langmuir* **12**, 5888 (1996).
- ⁷⁸ V. Buch, *J. Chem. Phys.* **100**, 7610 (1994).
- ⁷⁹ Q. Wang and J. K. Johnson, *Mol. Phys.* **95**, 299 (1998).
- ⁸⁰ Q. Wang and J. K. Johnson, *J. Chem. Phys.* **110**, 577 (1999).